

¹ PeriDEM – High-fidelity modeling of granular media consisting of deformable complex-shaped particles

³ Prashant K. Jha  ¹

⁴ 1 Department of Mechanical Engineering, South Dakota School of Mines and Technology, Rapid City,
⁵ SD 57701, USA

DOI: [10.xxxxxx/draft](https://doi.org/10.xxxxxx/draft)

Software

- [Review](#) 
- [Repository](#) 
- [Archive](#) 

Editor: [Open Journals](#) 

Reviewers:

- [@openjournals](#)

Submitted: 01 January 1970

Published: unpublished

License

Authors of papers retain copyright and release the work under a Creative Commons Attribution 4.0 International License ([CC BY 4.0](#))¹⁷¹⁸

⁶ Summary

⁷ Accurate simulation of granular materials under extreme mechanical conditions, such as crushing,
⁸ fracture, and large deformation, remains a significant challenge in geotechnical, manufacturing,
⁹ and mining applications. Classical discrete element method (DEM) models typically treat
¹⁰ particles as rigid or nearly rigid bodies, limiting their ability to capture internal deformation and
¹¹ fracture. The PeriDEM library, first introduced in ([Jha et al., 2021](#)), addresses this limitation
¹² by modeling particles as deformable solids using peridynamics, a nonlocal continuum theory
¹³ that naturally accommodates fracture and significant deformation. Inter-particle contact is
¹⁴ handled using DEM-inspired local laws, enabling realistic interaction between complex-shaped
¹⁵ particles.

¹⁶ Implemented in C++, PeriDEM is designed for extensibility and ease of deployment. It relies on a minimal set of external libraries, supports multithreaded execution, and includes demonstration examples involving compaction, fracture, and rotational dynamics. The framework facilitates granular-scale simulations, supports the development of constitutive models, and serves as a foundation for multi-fidelity coupling in real-world applications.

²¹ Statement of Need

²² Granular materials play a central role in many engineered systems, but modeling their behavior under high loading, deformation, and fragmentation remains an open problem. Popular open-source DEM codes such as YADE ([Smilauer et al., 2021](#)), BlazeDEM ([Govender et al., 2016](#)), Chrono DEM-Engine ([Zhang et al., 2024](#)), and LAMMPS ([Thompson et al., 2022](#)) are widely used but typically treat particles as rigid, limiting their accuracy in scenarios involving internal deformation and breakage. A recent review by Dosta et al. ([Dosta et al., 2024](#)) compares several DEM libraries. Meanwhile, peridynamics-based codes such as Peridigm ([Littlewood et al., 2024](#)) and NLMech ([Jha & Diehl, 2021](#)) are designed to simulate deformation and fracture within a single structure, with limited support for multi-structure simulations.

³¹ PeriDEM fills this gap by integrating state-based peridynamics for intra-particle deformation with DEM-style contact laws for particle interactions. This hybrid approach enables direct simulation of particle fragmentation, stress redistribution, and dynamic failure propagation—capabilities essential for modeling granular compaction, attrition, and crushing.

³⁵ Recent multiscale approaches, including DEM-continuum and DEM-level-set coupling methods ([Harmon et al., 2021](#)), aim to bridge scales but often rely on homogenization assumptions. Sand crushing in geotechnical systems, for example, has been modeled using micro-CT-informed FEM or phenomenological laws ([Chen et al., 2023](#)). PeriDEM offers a particle-resolved alternative that allows bottom-up investigation of granular failure and shape evolution, especially in systems where fragment dynamics are critical.

⁴¹ Brief Introduction to PeriDEM Model

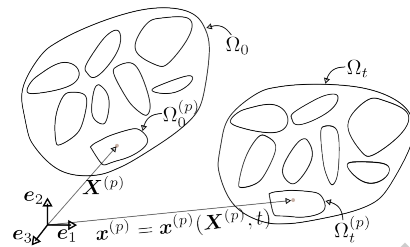


Figure 1: Motion of particle system.

⁴² Consider a fixed frame of reference and $\{e_i\}_{i=1}^d$ are orthonormal bases. Consider a collection
⁴³ of N_P particles $\Omega_0^{(p)}$, $1 \leq p \leq N_P$, where $\Omega_0^{(p)} \subset \mathbb{R}^d$ with $d = 2, 3$ represents the initial
⁴⁴ configuration of particle p . Suppose $\Omega_0 \supset \cup_{p=1}^{N_P} \Omega_0^{(p)}$ is the domain containing all particles; see
⁴⁵ Figure 1. The particles in Ω_0 are dynamically evolving due to external boundary conditions and
⁴⁶ internal interactions; let $\Omega_t^{(p)}$ denote the configuration of particle p at time $t \in (0, t_F]$, and
⁴⁷ $\Omega_t \supset \cup_{p=1}^{N_P} \Omega_t^{(p)}$ domain containing all particles at that time. The motion $x^{(p)} = x^{(p)}(\mathbf{X}^{(p)}, t)$
⁴⁸ takes point $\mathbf{X}^{(p)} \in \Omega_0^{(p)}$ to $x^{(p)} \in \Omega_t^{(p)}$, and collectively, the motion is given by $\mathbf{x} = \mathbf{x}(\mathbf{X}, t) \in$
⁴⁹ Ω_t for $\mathbf{X} \in \Omega_0$. We assume the media is dry and not influenced by factors other than
⁵⁰ mechanical loading (e.g., moisture and temperature are not considered). The configuration of
⁵¹ particles in Ω_t at time t depends on various factors, such as material and geometrical properties,
⁵² contact mechanism, and external loading. Essentially, there are two types of interactions
⁵³ present in the media:

- ⁵⁴ \blacksquare *Intra-particle interaction* that models the deformation and internal forces in the particle
⁵⁵ and
- ⁵⁶ \blacksquare *Inter-particle interaction* that accounts for the contact between particles and the boundary
⁵⁷ of the domain in which the particles are contained.

⁵⁸ In DEM, the first interaction is ignored, assuming that particle deformation is insignificant
⁵⁹ compared to inter-particle interactions. On the other hand, PeriDEM accounts for both
⁶⁰ interactions.

⁶¹ The balance of linear momentum for particle p , $1 \leq p \leq N_P$, takes the form:

$$\rho^{(p)} \ddot{\mathbf{u}}^{(p)}(\mathbf{X}, t) = \mathbf{f}_{int}^{(p)}(\mathbf{X}, t) + \mathbf{f}_{ext}^{(p)}(\mathbf{X}, t), \quad \forall (\mathbf{X}, t) \in \Omega_0^{(p)} \times (0, t_F), \quad (1)$$

⁶² where $\rho^{(p)}$, $\mathbf{f}_{int}^{(p)}$, and $\mathbf{f}_{ext}^{(p)}$ are density, and internal and external force densities. The
⁶³ above equation is complemented with initial conditions, $\mathbf{u}^{(p)}(\mathbf{X}, 0) = \mathbf{u}_0^{(p)}(\mathbf{X})$, $\dot{\mathbf{u}}^{(p)}(\mathbf{X}, 0) =$
⁶⁴ $\dot{\mathbf{u}}_0^{(p)}(\mathbf{X})$, $\mathbf{X} \in \Omega_0^{(p)}$.

⁶⁵ Internal force – State-based peridynamics

⁶⁶ The internal force term $\mathbf{f}_{int}^{(p)}(\mathbf{X}, t)$ in the momentum balance governs intra-particle deformation
⁶⁷ and fracture. In PeriDEM, this term is modeled using a simplified state-based peridynamics
⁶⁸ formulation that accounts for nonlocal interactions over a finite horizon. The underlying model
⁶⁹ and its numerical implementation are discussed in detail in ([Jha et al., 2021], Sections 2.1
⁷⁰ and 2.3].

⁷¹ DEM-inspired contact forces

⁷² The external force term $\mathbf{f}_{ext}^{(p)}(\mathbf{X}, t)$ includes body forces, wall-particle interactions, and contact
⁷³ forces from other particles. Contact is modeled using a spring-dashpot-slider formulation

74 applied locally when particles come within a critical distance; see [Figure 2](#). This approach
 75 introduces nonlinear normal forces, damping, and friction without relying on particle convexity
 76 or geometric simplifications. The full formulation of contact detection, force assembly, and
 77 implementation is detailed in [[\(Jha et al., 2021\)](#), Section 2.2].

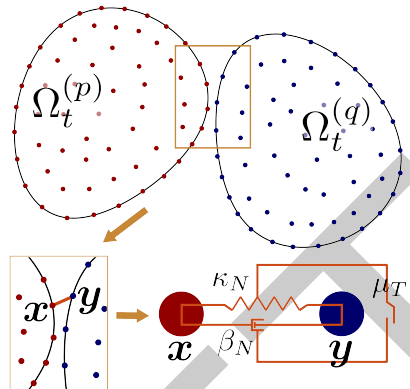


Figure 2: High-resolution contact approach in PeriDEM model for granular materials between arbitrarily-shaped particles. The spring-dashpot-slider system shows the normal contact (spring), normal damping (dashpot), and tangential friction (slider) forces between points x and y .

78 Implementation

79 [PeriDEM](#) is implemented in C++ and hosted on GitHub. It depends on a minimal set of external
 80 libraries, most of which are bundled in the external directory. Key dependencies include
 81 Taskflow ([Huang et al., 2021](#)) for multithreaded parallelism, nanoflann ([Blanco & Rai, 2014](#))
 82 for efficient neighborhood search, and VTK for output. The numerical strategies for neighbor
 83 search, peridynamic integration, damage evaluation, and time stepping follow those introduced
 84 in [[\(Jha et al., 2021\)](#), Section 3]. The core simulation model is implemented in `src/model/dem`,
 85 with the class `DEMModel` managing particle states, force calculations, and time integration.
 86 This work builds on earlier research in the analysis and numerical methods for peridynamics;
 87 see ([Jha et al., 2025; Jha & Lipton, 2018a, 2018b, 2019; Jha & Lipton, 2020](#)).

88 Features

- 89 ▪ Combines peridynamics and DEM to model intra-particle deformation and inter-particle
 90 contact
- 91
- 92 ▪ Simulates deformation and breakage of single particles under complex loading conditions
- 93
- 94 ▪ Supports arbitrarily shaped particles for realistic granular systems
- 95
- 96 ▪ Ongoing development of MPI-based parallelism and adaptive modeling strategies to
 97 improve efficiency without sacrificing accuracy

98 Examples

99 Example cases are described in [examples/README.md](#). One key simulation demonstrates
 100 the compression of over 500 circular and hexagonal particles in a rectangular container by
 101 displacing the top wall. The stress on the wall becomes increasingly nonlinear with penetration
 102 depth as damage accumulates and the medium yields (see [Figure 3a](#)).

103 Preliminary performance tests show that compute time increases exponentially with particle
 104 count due to the nonlocal nature of both peridynamic and contact interactions—highlighting

105 a computational bottleneck. This motivates future integration of MPI-based parallelism and
 106 a multi-fidelity modeling framework. Additional examples include attrition of non-circular
 107 particles in a rotating cylinder (Figure 3c).

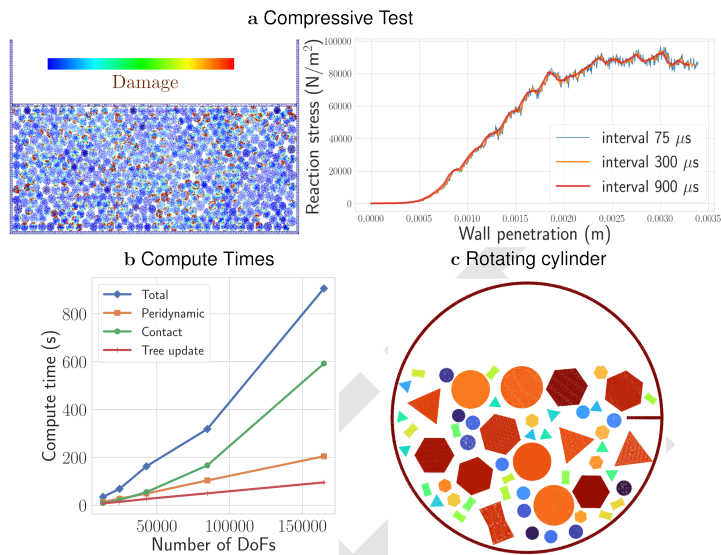


Figure 3: (a) Nonlinear response under compression, (b) exponential growth of compute time due to nonlocality of internal and contact forces, and (c) rotating cylinder with nonspherical particles.

108 Acknowledgements

109 This work was supported by the U.S. National Science Foundation through the Engineering
 110 Research Initiation (ERI) program under Grant No. 2502279. The support has contributed to
 111 the continued development and enhancement of the PeriDEM library.

112 References

- 113 Blanco, J. L., & Rai, P. K. (2014). *Nanoflann: A C++ header-only fork of FLANN, a library*
 114 *for nearest neighbor (NN) with KD-trees*. <https://github.com/jlblancoc/nanoflann>.
- 115 Chen, Q., Li, Z., Dai, Z., Wang, X., Zhang, C., & Zhang, X. (2023). Mechanical behavior and
 116 particle crushing of irregular granular material under high pressure using discrete element
 117 method. *Scientific Reports*, 13(1), 7843. <https://doi.org/10.1038/s41598-023-35022-w>
- 118 Dosta, M., André, D., Angelidakis, V., Caulk, R. A., Celigueta, M. A., Chareyre, B., Dietiker, J.-
 119 F., Girardot, J., Govender, N., Hubert, C., & others. (2024). Comparing open-source DEM
 120 frameworks for simulations of common bulk processes. *Computer Physics Communications*,
 121 296, 109066. <https://doi.org/10.1016/j.cpc.2023.109066>
- 122 Govender, N., Wilke, D. N., & Kok, S. (2016). Blaze-DEMGPU: Modular high performance
 123 DEM framework for the GPU architecture. *SoftwareX*, 5, 62–66. <https://doi.org/10.1016/j.softx.2016.04.004>
- 125 Harmon, J. M., Karapiperis, K., Li, L., Moreland, S., & Andrade, J. E. (2021). Modeling
 126 connected granular media: Particle bonding within the level set discrete element method.
 127 *Computer Methods in Applied Mechanics and Engineering*, 373, 113486. <https://doi.org/10.1016/j.cma.2020.113486>
- 129 Huang, T.-W., Lin, D.-L., Lin, C.-X., & Lin, Y. (2021). Taskflow: A lightweight parallel and

- 130 heterogeneous task graph computing system. *IEEE Transactions on Parallel and Distributed
131 Systems*, 33(6), 1303–1320. <https://doi.org/10.1109/TPDS.2021.3104255>
- 132 Jha, P. K., Desai, P. S., Bhattacharya, D., & Lipton, R. (2021). Peridynamics-based discrete
133 element method (PeriDEM) model of granular systems involving breakage of arbitrarily
134 shaped particles. *Journal of the Mechanics and Physics of Solids*, 151, 104376. <https://doi.org/10.1016/j.jmps.2021.104376>
- 135 Jha, P. K., & Diehl, P. (2021). NLMech: Implementation of finite difference/meshfree
136 discretization of nonlocal fracture models. *Journal of Open Source Software*, 6(65), 3020.
137 <https://doi.org/10.21105/joss.03020>
- 138 Jha, P. K., Diehl, P., & Lipton, R. (2025). Nodal finite element approximation of peridynamics.
139 *Computer Methods in Applied Mechanics and Engineering*, 434, 117519. <https://doi.org/10.1016/j.cma.2024.117519>
- 140 Jha, P. K., & Lipton, R. (2018a). Numerical analysis of nonlocal fracture models in holder
141 space. *SIAM Journal on Numerical Analysis*, 56(2), 906–941. <https://doi.org/10.1137/17M112236>
- 142 Jha, P. K., & Lipton, R. (2018b). Numerical convergence of nonlinear nonlocal continuum
143 models to local elastodynamics. *International Journal for Numerical Methods in Engineering*,
144 114(13), 1389–1410. <https://doi.org/10.1002/nme.5791>
- 145 Jha, P. K., & Lipton, R. (2019). Numerical convergence of finite difference approximations for
146 state based peridynamic fracture models. *Computer Methods in Applied Mechanics and
147 Engineering*, 351, 184–225. <https://doi.org/10.1016/j.cma.2019.03.024>
- 148 Jha, P. K., & Lipton, R. P. (2020). Kinetic relations and local energy balance for LEFM from
149 a nonlocal peridynamic model. *International Journal of Fracture*. <https://doi.org/10.1007/s10704-020-00480-0>
- 150 Littlewood, D. J., Parks, M. L., Foster, J. T., Mitchell, J. A., & Diehl, P. (2024). The
151 peridigm meshfree peridynamics code. *Journal of Peridynamics and Nonlocal Modeling*,
152 6(1), 118–148. <https://doi.org/10.1007/s42102-023-00100-0>
- 153 Smilauer, V., Angelidakis, V., Catalano, E., Caulk, R., Chareyre, B., Chèvremont, W., Doro-
154 feenko, S., Duriez, J., Dyck, N., Elias, J., Er, B., Eulitz, A., Gladky, A., Guo, N., Jakob, C.,
155 Kneib, F., Kozicki, J., Marzougui, D., Maurin, R., ... Yuan, C. (2021). Yade documentation
156 (3rd edition). *Zenodo*. <https://doi.org/10.5281/zenodo.5705394>
- 157 Thompson, A. P., Aktulga, H. M., Berger, R., Bolintineanu, D. S., Brown, W. M., Crozier, P.
158 S., in 't Veld, P. J., Kohlmeyer, A., Moore, S. G., Nguyen, T. D., Shan, R., Stevens, M. J.,
159 Tranchida, J., Trott, C., & Plimpton, S. J. (2022). LAMMPS - a flexible simulation tool for
160 particle-based materials modeling at the atomic, meso, and continuum scales. *Computer
161 Physics Communications*, 271, 108171. <https://doi.org/10.1016/j.cpc.2021.108171>
- 162 Zhang, R., Tagliafierro, B., Vanden Heuvel, C., Sabarwal, S., Bakke, L., Yue, Y., Wei, X.,
163 Serban, R., & Negruț, D. (2024). Chrono DEM-Engine: A discrete element method dual-
164 GPU simulator with customizable contact forces and element shape. *Computer Physics
165 Communications*, 300, 109196. <https://doi.org/10.1016/j.cpc.2024.109196>
- 166
- 167
- 168
- 169